Contents lists available at ScienceDirect

Theoretical and Applied Fracture Mechanics

journal homepage: http://ees.elsevier.com

Effect of grain size on the very high cycle fatigue behavior and notch sensitivity of titanium

S.V. Sajadifar [a,b,*], T. Wegener [a], G.G. Yapici [b], T. Niendorf [a]

[a] Universität Kassel, Institut für Werkstofftechnik (Materials Engineering), 34125 Kassel, Germany
[b] Mechanical Engineering Department, Ozyegin University, 34794 Istanbul, Turkey

ARTICLE INFO

Keywords
Ultra-fine grained titanium
Equal channel angular extrusion/pressing
Very high-cycle fatigue
Severe plastic deformation
Notch sensitivity
Fracture morphology

ABSTRACT

The very high-cycle fatigue performances of coarse-grained and ultrafine-grained titanium samples with different geometries at ambient temperature and various stress amplitudes were investigated. Severe plastic deformation improves monotonic strength of titanium at the cost of a loss in ductility. Ultrafine-grained titanium demonstrates a superior fatigue performance compared to that of coarse-grained counterparts in the high-cycle fatigue regime, however, suffers notch sensitivity. Furthermore, in the very high-cycle fatigue regime stress-life curves merge unexpectedly. Microstructural inhomogeneity in the ultrafine-grained titanium is expected to be the reason. Analysis of fracture surfaces reveals that the formation of fatigue slip marks is evident on the fatigued samples of both microstructural states. Ultrafine-grained titanium is more prone to the intergranular fracture.

1. Introduction

Commercial purity titanium (Ti) is an exceptional candidate for engineering applications requiring the combination of strength and ductility along with good biocompatibility. Former studies showed that grain refinement via severe plastic deformation (SPD) is capable of enhancing the strength of Ti [1,2]. Equal channel angular extrusion/pressing (ECAE/P) was found to be the most promising SPD method for achieving ultrafine-grained (UFG) microstructure and improving strength of Ti [3]. Improvement of monotonic mechanical properties of Ti after ECAE was a topic of interest in several studies [4,5,14,15,6–13]. Monotonic deformation response of UFG Ti was comprehensively investigated at ambient temperature [6–10]. Besides, the elevated temperature behavior of this material was probed under monotonic loading [11–15]. Accordingly, flow stress levels of UFG Ti were higher than those of coarse-grained (CG) counterparts at or below 600 °C, while the influence of grain refinement was seen to be degraded due to grain growth at higher deformation temperature.

Investigating monotonic behavior of severely deformed Ti was not the only goal of research works. Since many envisaged engineering components, e.g. in the biomedical industry, typically experience cyclic loads, exploring the fatigue behavior of UFG Ti is very important. Thus, performance under cyclic loading of UFG materials in general and UFG Ti in particular draw the attention of many researchers in recent years [16–18]. Especially, the demand for obtaining high fatigue strength and lives of Ti has driven investigations on the cyclic response of this material in various conditions [19–22]. In spite of several studies focusing on low- and high-cycle fatigue (LCF and HCF) behavior of UFG Ti [17–22], the cyclic performance of this material in the very high cycle fatigue (VHCF) regime has not been discussed hitherto. Data available reporting on the VHCF performance of other UFG materials such as Cu- and Al-alloys reveal an improvement in fatigue performance [16,23–25]. For UFG Al-based alloys it has been reported that "the strength of the weakest microstructural detail and the area of maximum localized plastic deformation determine the crack initiation sites in the VHCF regime" [16]. In how far this holds true for UFG Ti having a different lattice structure and, thus, fundamentally different slip behavior remains unclear so far. Besides, the effect of notch sensitivity on the HCF and VHCF response of UFG Ti has not been addressed, yet. A notch, i.e. a discontinuity in shape, leads to locally increased stresses promoting fatigue crack initiation. The general properties of UFG materials, i.e. high initial strength and limited strain hardening capability, could impede plasticity induced redistribution of stress peaks in direct vicinity of notches. This concomitantly should lead to increased notch sensitivity, which indeed has been shown for other UFG materials such as UFG Cu [26]. However, again the different lattice structure of UFG

* Corresponding author at: Universität Kassel, Institut für Werkstofftechnik (Materials Engineering), 34125 Kassel, Germany.
E-mail address: sajjadifar@uni-kassel.de (S.V. Sajadifar)

https://doi.org/10.1016/j.tafmec.2019.102362
Received 18 March 2019; Received in revised form 10 July 2019; Accepted 15 September 2019
Available online xxx
0167-8442/

Ti hinders straightforward interpretation of results available in the literature.

Therefore, the aim of this investigation is to study the cyclic stability of ECAE processed Ti with varying geometries in the HCF and VHCF regimes. In this quest, fatigue response and fatigue crack initiation mechanism of CG and UFG grade 4 Ti tested at a frequency of 1 kHz and various stress amplitudes are presented. The results reveal that samples with smooth geometry and UFG microstructure showed the best fatigue performance in the VHCF regime. Microstructure analysis revealed the formation of cyclic slip markings on the surfaces of CG and UFG fatigued specimens being linked to the initiation of cracks.

2. Material and methods

Commercial purity grade 4 Ti billets were coated with a graphite-based lubricant before extrusion. Afterward, the bars were heated in a furnace where they were held for 1 h before extrusion. The minimum deformation temperature that allowed for processing without shear localization and macroscopic cracking for a 90° ECAE die was determined to be 450 °C. Extrusion rate was about 1.27 mm/s. Eight ECAE passes were conducted following route B_C accumulating a total strain of 9.24 in the as-processed material. In route B_C the billet was rotated by +90° around its long axis between each successive pass. The schematic diagram of ECAE route B_C is shown in Fig. 1. After each extrusion pass, the billets were water quenched to preserve the microstructure achieved during ECAE. Route B_C was selected as the ECAE processing route resulting in the highest volume fraction of high-angle grain boundaries as well as best microstructural homogeneity and, thus, superior monotonic properties for the UFG Ti considered [8].

Tensile tests were conducted on flat dog-bone shaped samples with gauge section dimensions of 8 mm × 3 mm × 1.5 mm at ambient temperature using an MTS793 test rig in displacement control with a crosshead speed of 2 mm/min corresponding to a nominal strain rate of 0.004 s^{-1} (calculated on basis of the sample gauge length). VHCF experiments were performed employing 2 mm thick flat dog-bone shaped samples with two different geometries as shown in Fig. 2. All samples were ground and polished to eliminate major scratches and minimize the effect of the residual layer from electro-discharge machining (EDM). Cyclic tests were carried out at various stress amplitudes and at ambient temperature. A RUMUL GIGAFORTE resonant testing machine was used to perform fatigue experiments at 1000 Hz. Fatigue experiments were conducted under fully reversed push-pull loading at constant total stress amplitude (R = −1). Forced convection was utilized to cool down the specimens during the VHCF experiments and maintain the temperature within the gauge length close to ambient temperature. Thermocouples were used to measure the temperature of the samples

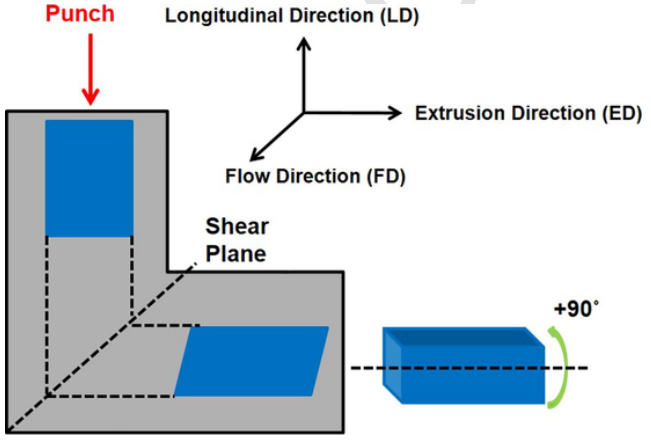

Fig. 1. Schematic diagram of route B_C processing for ECAE.

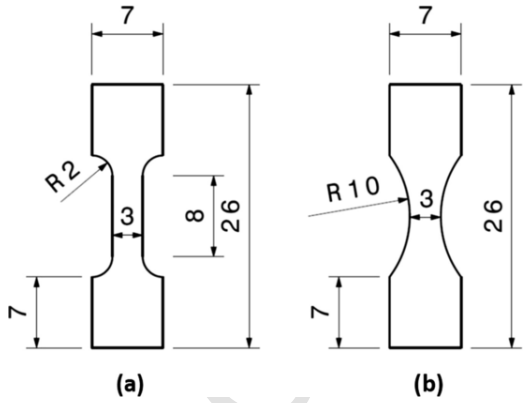

Fig. 2. Geometry of the very high-cycle fatigue specimens used in the present study (a) sample with a radius of 2 mm and (b) sample with radius of 10 mm.

during cyclic loading. Scanning electron microscopy (SEM) at an accelerating voltage of 20 kV and electron backscatter diffraction (EBSD) were utilized for analyzing the relevant damage mechanisms. For EBSD examination, the samples were further prepared by 48 h of vibro-polishing using a conventional oxide polishing suspension (OPS).

3. Results and discussion

3.1. Microstructural evolution and tensile properties

Microstructures of both CG and UFG Ti are displayed in Fig. 3. The EBSD grain map of the UFG Ti sample was recorded from the transverse plane. Evidently, 8 passes of ECAE processing were capable of manufacturing Ti with UFG microstructure. The average grain sizes of CG and UFG Ti were measured to be 46 μm and 300 nm, respectively. The grain sizes were determined based on the linear intercept method.

Before studying behavior of CG and UFG Ti under cyclic loading, monotonic responses of both microstructural states were characterized by performing tensile tests. Ambient temperature tensile engineering stress-strain curves of both CG and UFG Ti are demonstrated in Fig. 4. SPD could enhance the yield and tensile strengths of Ti despite a noticeable loss in ductility. The improvement of flow strength after SPD is attributed to the effect of the dislocation substructure and the high density of grain boundaries (GBs) [1,27].

3.2. Fatigue performance

S-N curves of both CG and UFG Ti are shown in Fig. 5. The way of presentation allows for direct evaluation of the notch sensitivity of CG and UFG Ti. For both conditions, number of cycles to failure continuously decreases with the increase of the stress amplitude. This can be imputed to the acceleration of crack initiation and subsequent growth of the resulting cracks. The results reveal that specimens with a larger radius (smoother geometry) show a better fatigue performance. This has been expected and is in line with literature. It is well-known that the fatigue endurance of samples with smoother geometry is much higher than that of less smooth ones [20,21,28]. This could be rationalized in terms of relatively low fatigue stress concentrations in smooth specimens. However, the fatigue performance revealed in Fig. 5 opens up some questions. The difference for samples in the CG condition is not strongly pronounced and overlaid by the general scatter. The fatigue notch factor at a given number of cycles to failure N_f can be calculated as [29]:

$$K_f = \sigma_{a,\,smooth}/\sigma_{a,\,notch}$$

In the equation above, σa, smooth and σ_a, notch are the fatigue amplitudes of smooth and notched samples, respectively. Considering the

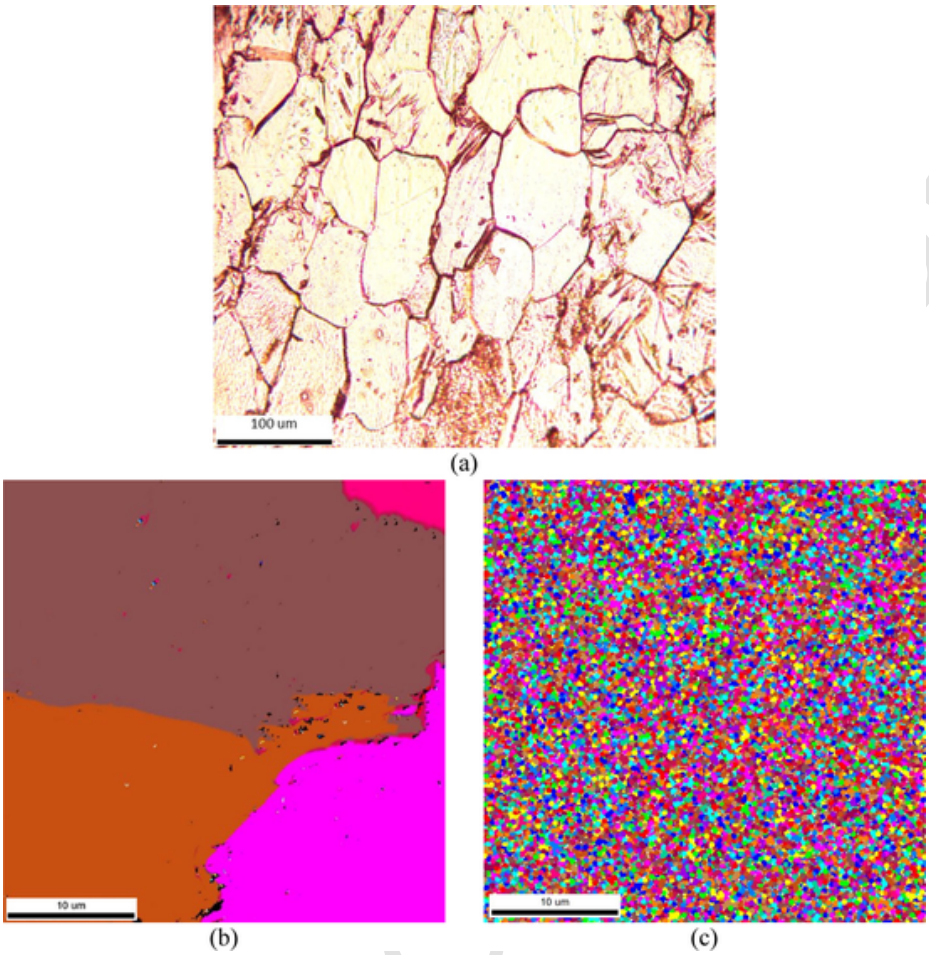

Fig. 3. (a) Optical micrograph of CG Ti; EBSD grain maps of (b) CG Ti, and (c) UFG Ti.

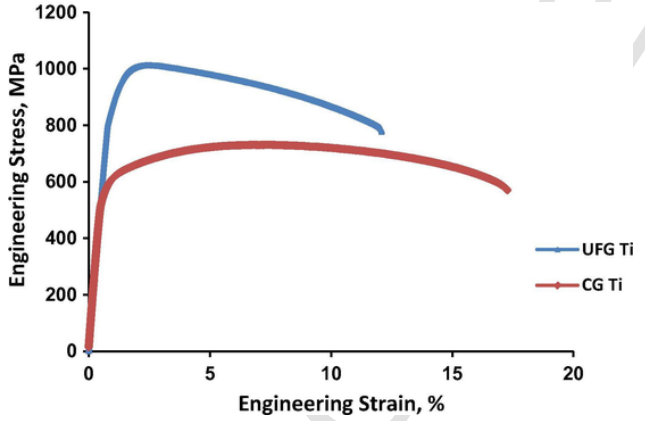

Fig. 4. Ambient temperature tensile engineering stress-strain curves of CG and UFG Ti.

R10 and the R2 samples as smooth and notched conditions, the fatigue notch factors of CG and UFG Ti (evaluated at the number of cycles to failure of 10^6) were calculated to be 1.01 and 1.22 based on the trend lines plotted in Fig. 5. Hence, notch effects in the relatively ductile CG condition are seen to be not pronounced, especially as the R2 sample is still not severely notched. On the contrary, the fatigue resistance of UFG Ti is affected by specimen geometry. Again, fatigue lives for given stress amplitudes are always higher for the specimens featuring the smooth geometry, i.e. the radius R10. In the case of the UFG Ti, the slope of both trendlines (lines) is different, however, not as pronounced as initially expected. This already indicates that even at low-amplitude loading microstructural features being present in the UFG Ti, e.g. inhomogeneities stemming from non-perfect material flow during ECAE [30], promote crack initiation even in the absence of a geometrical notch. As those inhomogeneities are expected to be distributed all over the gauge section of the samples, geometrical notches still can additionally be effective in deteriorating the fatigue performance of the UFG Ti by promoting damage evolution by a general increase of the stress level in direct vicinity of the notch, as e.g. shown for UFG Cu [26].

Another factor is expected to contribute to the total fatigue lives determined. Generally, fatigue lives of the notched samples are strongly dominated by their crack propagation resistance, which can be postponed for ductile materials [21]. SPD processing leads to the reduction in ductility, hence crack propagation resistance is degraded [31]. As in Fig. 5 only CG and UFG material are evaluated separately, this difference has not been taken into account here, however, will be considered in the following discussion.

Fig. 6 represents the comparison between UFG and CG Ti S-N plots for samples with radii of 2 mm (Fig. 6a) and 10 mm (Fig. 6b). Obviously, SPD processing is capable of substantially enhancing the HCF performance of Ti. This improvement is more pronounced for the samples with smoother geometry (Fig. 6b) again revealing a higher notch sensitivity of the UFG Ti, which has been already reported before [20,28]. Increase in monotonic strength is known to be very effective in improving the resistance to crack initiation and, therefore, a better fatigue performance is expected in severely deformed Ti with its higher strength [21]. Such kind of enhancement of fatigue endurance in the HCF and VHCF regimes was already reported for UFG copper [23,24] and UFG Al-alloys [16,25]. In the results shown for the UFG Ti in Fig.

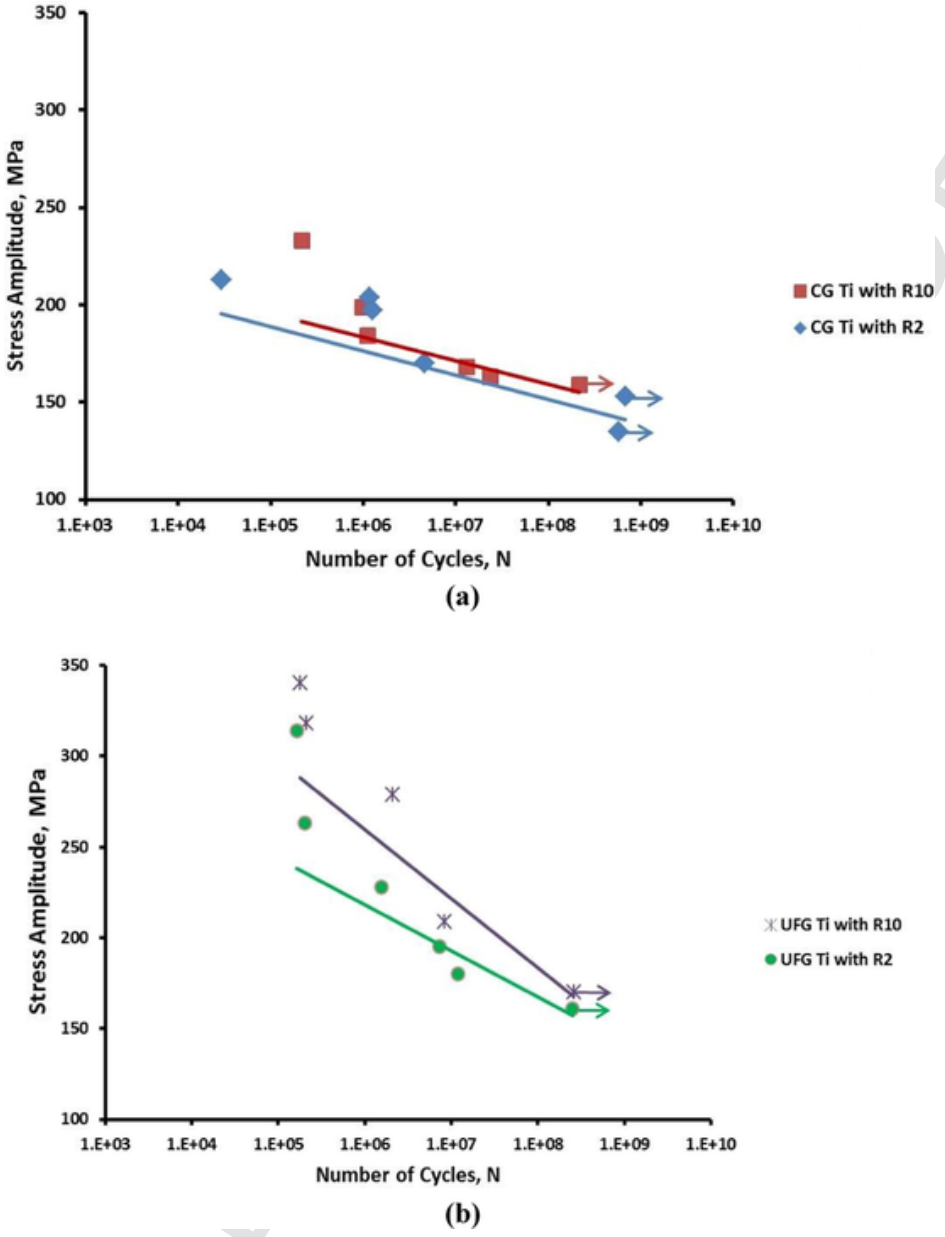

Fig. 5. S-N curves for (a) CG Ti and (b) UFG Ti tested with different geometries.

6, however, a different behavior for the VHCF regime can be seen. For both the unnotched and the notched samples the trendlines merge at very high number of cycles to failure. In light of the results presented in the literature, this had not been expected. The following aspects have to be considered for evaluating the results shown: (1) Ti is characterized by a hexagonal lattice structure and, thus, shows a different slip behavior as compared to Al- and Cu-alloys; (2) Even upon ECAE processing using the most efficient route B_C, microstructural inhomogeneities on the local scale cannot be fully avoided (as will be shown in the final part of this section); (3) Total fatigue life is the sum of crack initiation life and crack propagation life, the latter being clearly inferior in terms of UFG materials [31–33]; (4) Elementary mechanisms being responsible for crack initiation in the HCF and the VHCF regime are different [34]. Based on these considerations the unexpectedly low fatigue strength of the UFG Ti in the VHCF regime can be explained as follows: In accordance with the findings for UFG Al-alloys [16,25], the weakest microstructural feature determines the VHCF performance of the alloy. The microstructural inhomogeneities in the UFG Ti act as microstructural notches in a similar way as has been shown for UFG interstitial-free steel in a series of papers [35,36]. As Ti is hard to deform even at the applied ECAE processing temperatures, such inhomogeneities prevail in numerous regions of the UFG sample (cf. Fig. 6b and the corresponding discussion in the next paragraphs). Due to the stress rising effect of these structures, local slip activities are promoted leading to relatively fast crack initiation even at very low absolute stress amplitudes. As crack growth then is strongly promoted due to the UFG microstructure [31,37], total fatigue lives of UFG and CG Ti converge in the VHCF regime. Microstructural analysis presented in the following promotes this schematic fatigue model.

An EBSD micrograph (inverse pole figure (IPF) plot) of severely deformed Ti upon very high-cycle fatigue testing is provided in Fig. 6. Obviously, no grain coarsening occurred during the VHCF tests, even at the highest strain amplitude. Based on these results, grain coarsening can be excluded as the damage mechanism in UFG Ti during ambient temperature cyclic response. Grain coarsening also was not observed for UFG copper following VHCF testing [23].

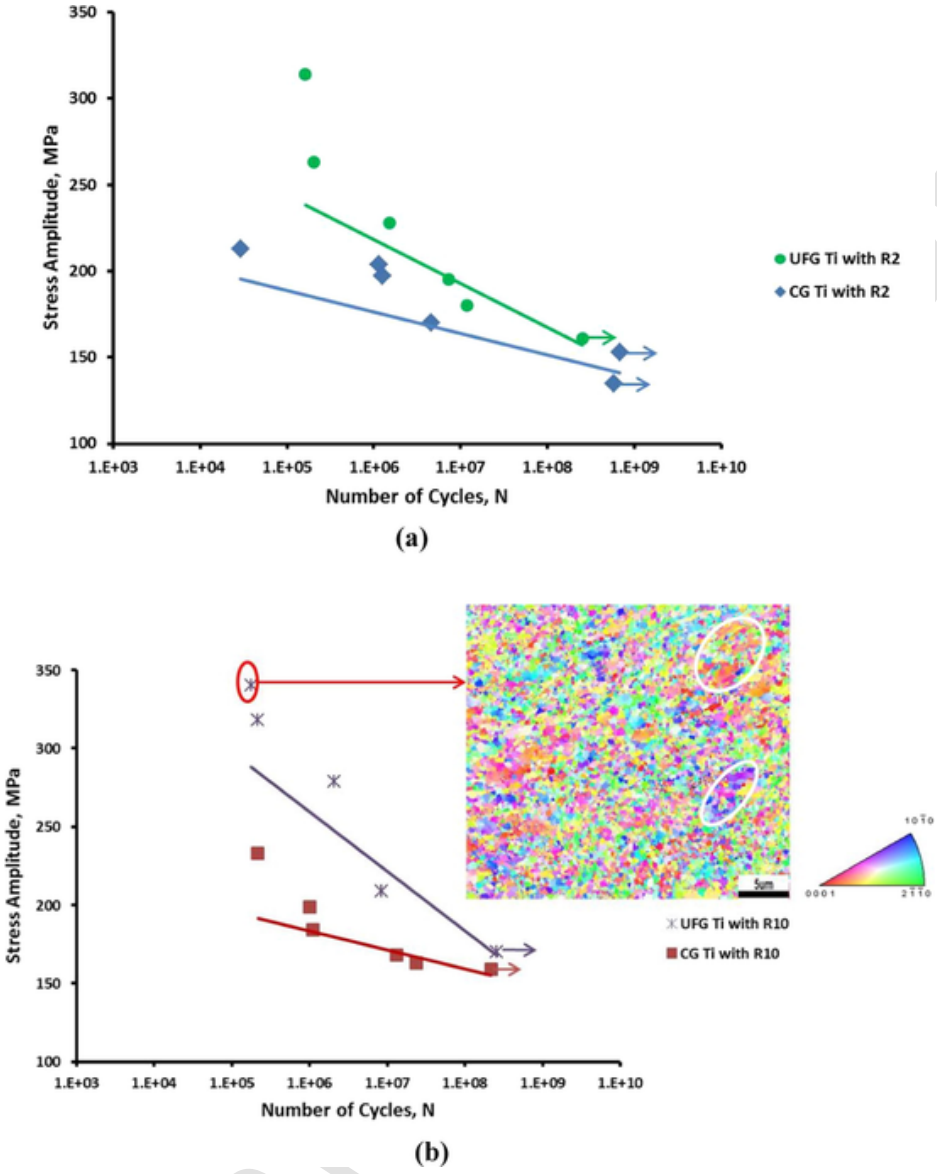

Fig. 6. S-N curves of CG and UFG Ti for samples with radii of (a) 2 mm and (b) 10 mm. The EBSD inverse pole figure (IPF) map of a fatigued UFG Ti specimen (stress amplitude of 340 MPa) is shown on the right.

The EBSD micrograph shown in Fig. 6 obtained in the gauge length of the specimen reveals the presence of clusters of grains with similar orientation (two clusters are highlighted by white circles). Based on the EBSD observations reported in UFG IF steel literature, such clusters act as microstructural notches during cyclic loading [35,36,38]. The cyclic response of Ti could be even more sensitive to these clusters and inhomogeneities due to its different lattice structure and deformation mechanisms [39,40]. Thus, observations reported in the present work and cited papers clearly indicate that the main reason for relatively fast crack initiation even at very low absolute stress amplitudes in the UFG structure can be rationalized based on the presence of microstructural inhomogeneities, i.e. clusters of grains. It is also worth noting that microtextured regions (MTRs) have a profound effect on crack initiation in Ti alloys [41–45]. In this case, each MTR consists of clusters of semi-random grain orientations. The maximum localized plastic deformation was shown to take place within MTRs that enabled slip transmission across grains with low-angle boundaries [41].

3.3. Fractography

With the aim of studying the cyclic behavior and fracture mechanisms in the VHCF regime, selected samples were further investigated by SEM. Evolution of surface morphologies on initially polished surfaces of specimens tested at different stress amplitudes is shown in Fig. 7. Sample surfaces of both fatigued UFG and CG Ti show the formation of fatigue slip marks and cracks on the fatigued specimens as highlighted by arrows in Fig. 7a, c, and e. In the VHCF regime, stress amplitudes are chosen to be below a threshold for formation of slip marks such as e.g. persistent slip bands (PSBs). However, due to local stress concentration, e.g. at microstructure inhomogeneities, the formation of the threshold can be exceeded in these regions eventually leading to final fracture of the sample. Lukas et al. [23] recently observed the initiation of PSBs in UFG copper upon VHCF testing. In consequence, presence of slip marks on the sample surfaces in the current study reveals dislocation activity in the UFG Ti tested at even lowest stress amplitudes and, thus, provides a rationale for the course of damage as intro-

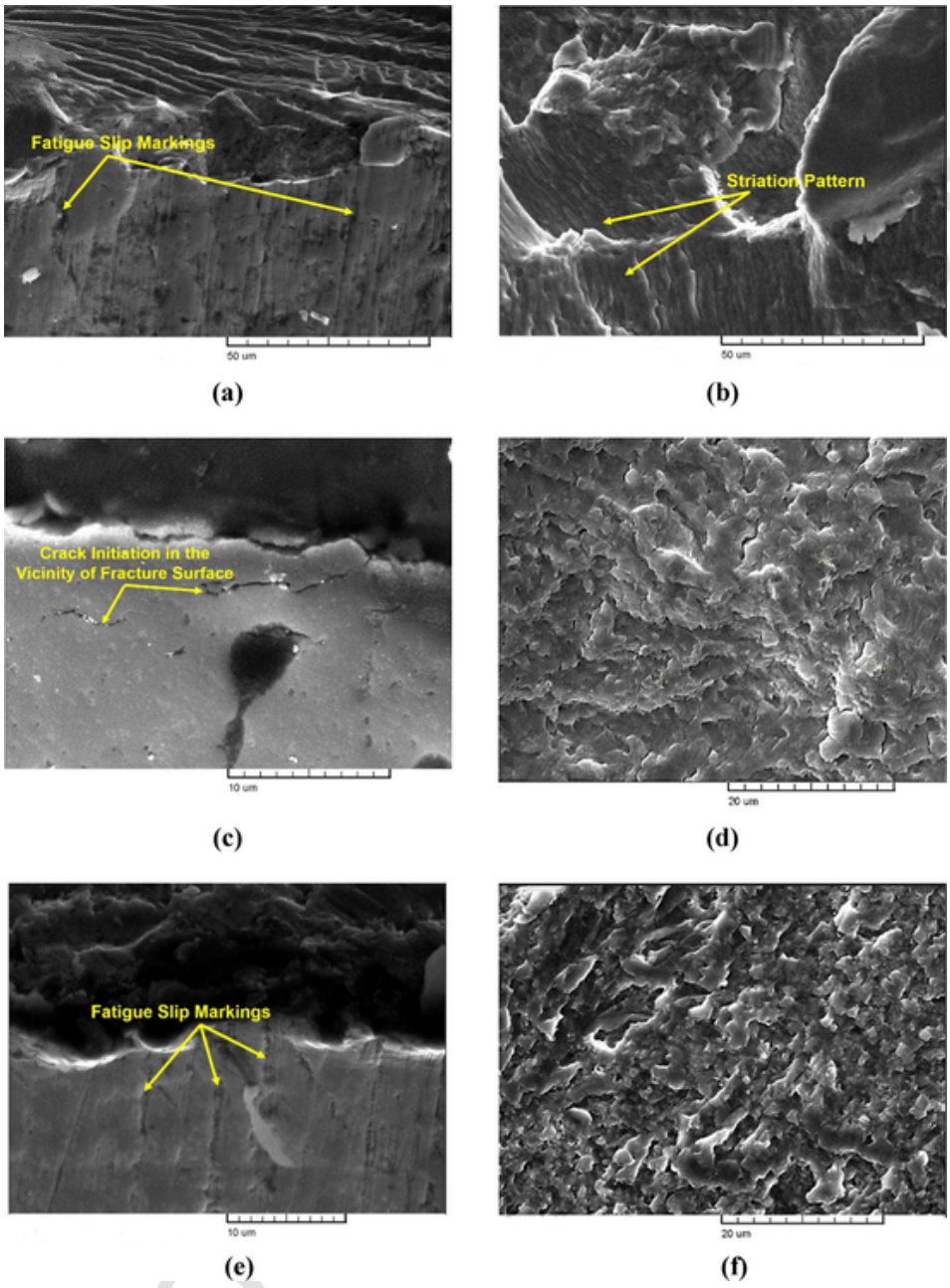

Fig. 7. Side and fracture surfaces of the specimens; (a) frontal view of CG Ti with R2 fatigued at a stress amplitude of 170 MPa, (b) fracture surface of CG Ti with R10 fatigued at a stress amplitude of 233 MPa, (c) frontal view of UFG Ti with R10 fatigued at a stress amplitude of 290 MPa, (d) fracture surface of UFG Ti with R2 fatigued at a stress amplitude of 314 MPa (e) frontal view of UFG Ti with R2 fatigued at a stress amplitude of 314 MPa and (f) fracture surface of UFG Ti with R10 fatigued at a stress amplitude of 340 MPa.

duced and discussed above, and finally the unexpected low fatigue strength of the UFG Ti in the VHCF regime.

Analysis of fracture surfaces provides further insights into damage evolution. A typical fracture surface revealing striations and clamshell mark patterns is seen for CG Ti (Fig. 7b). By contrast, intergranular fracture is seen on the fracture surfaces for the UFG Ti fatigued specimens as shown in Fig. 7d and f. Energy-wise, intergranular fracture is more favorable than transgranular fracture in UFG materials considering that they contain higher volume fraction of grain boundaries [19] eventually leading to low resistance towards crack growth. A similar fracture morphology was also shown for UFG Ti tested under traditional high-cycle fatigue loading [19].

4. Conclusions

In the present study, the influence of grain size on the VHCF behavior of titanium was studied with an emphasis on notch sensitivity. ECAE processing enhances the monotonic strength of grade 4 titanium at ambient temperature due to its UFG structure. Under cyclic loading, UFG Ti demonstrated relatively higher sensitivity to the specimen geometry. UFG Ti showed a better fatigue performance and endurance in the HCF regime, attesting the improvement of mechanical strength via SPD processing resulting in higher resistance to crack nucleation. However, in the VHCF fatigue at very high number of cycles to failure fatigue performances of CG and UFG Ti converge. In this regime microstructural inhomogeneities, being present in the UFG Ti, act as microstructural notches and, thus, stress raisers facilitating local slip ac-

tivity and finally premature crack initiation.

Acknowledgements

The authors thank the Hessen State Ministry of Higher Education, Research and the Arts – Initiative for the Development of Scientific and Economic Excellence (LOEWE) – for financial support through the research project 'Safer Materials'.

References

[1] Z. Fan, H. Jiang, X. Sun, J. Song, X. Zhang, C. Xie, Microstructures and mechanical deformation behaviors of ultrafine-grained commercial pure (grade 3) Ti processed by two-step severe plastic deformation, Mater. Sci. Eng. A. 527 (2009) 45–51, doi:10.1016/j.msea.2009.07.030.
[2] G.G. Yapici, I. Karaman, H.J. Maier, Mechanical flow anisotropy in severely deformed pure titanium, Mater. Sci. Eng. A 434 (2006) 294–302, doi:10.1016/j.msea.2006.06.082.
[3] B. Altan, Severe plastic deformation : toward bulk production of nanostructured materials, Nova Sci. (2006).
[4] S. Faghihi, F. Azari, A.P. Zhilyaev, J.A. Szpunar, H. Vali, M. Tabrizian, Cellular and molecular interactions between MC3T3-E1 pre-osteoblasts and nanostructured titanium produced by high-pressure torsion, Biomaterials 28 (2007) 3887–3895, doi:10.1016/j.biomaterials.2007.05.010.
[5] J.C. Fonseca, G.E.P. Henriques, L.C. Sobrinho, M.F. de Góes, Stress-relieving and porcelain firing cycle influence on marginal fit of commercially pure titanium and titanium-aluminum-vanadium copings, Dent. Mater. 19 (2003) 686–691 (accessed January 19, 2017). http://www.ncbi.nlm.nih.gov/pubmed/12901996.
[6] J.L. Milner, F. Abu-Farha, C. Bunget, T. Kurfess, V.H. Hammond, Grain refinement and mechanical properties of CP-Ti processed by warm accumulative roll bonding, Mater. Sci. Eng. A. 561 (2013) 109–117, doi:10.1016/j.msea.2012.10.081.
[7] C.T. Wang, N. Gao, M.G. Gee, R.J.K. Wood, T.G. Langdon, Processing of an ultrafine-grained titanium by high-pressure torsion: an evaluation of the wear properties with and without a TiN coating, J. Mech. Behav. Biomed. Mater. 17 (2013) 166–175, doi:10.1016/j.jmbbm.2012.08.018.
[8] V.V. Stolyarov, Y.T. Zhu, I.V. Alexandrov, T.C. Lowe, R.Z. Valiev, Influence of ECAP routes on the microstructure and properties of pure Ti, Mater. Sci. Eng. A. 299 (2001) 59–67, doi:10.1016/S0921-5093(00)01411-8.
[9] R.E. Barber, T. Dudo, P.B. Yasskin, K.T. Hartwig, Product yield for ECAE processing, Scr. Mater. 51 (2004) 373–377, doi:10.1016/j.scriptamat.2004.05.022.
[10] S. Suwas, B. Beausir, L.S. Tóth, J.J. Fundenberger, G. Gottstein, Texture evolution in commercially pure titanium after warm equal channel angular extrusion, Acta Mater. 59 (2011) 1121–1133, doi:10.1016/j.actamat.2010.10.045.
[11] V.L. Sordi, M. Ferrante, M. Kawasaki, T.G. Langdon, Microstructure and tensile strength of grade 2 titanium processed by equal-channel angular pressing and by rolling, J. Mater. Sci. 47 (2012) 7870–7876, doi:10.1007/s10853-012-6593-x.
[12] S.V. Sajadifar, G.G. Yapici, Elevated temperature mechanical behavior of severely deformed titanium, J. Mater. Eng. Perform. 23 (2014) 1834–1844, doi:10.1007/s11665-014-0947-2.
[13] H. Shahmir, P.H.R. Pereira, Y. Huang, T.G. Langdon, Mechanical properties and microstructural evolution of nanocrystalline titanium at elevated temperatures, Mater. Sci. Eng. A 669 (2016) 358–366, doi:10.1016/j.msea.2016.05.105.
[14] S.V. Sajadifar, G.G. Yapici, Workability characteristics and mechanical behavior modeling of severely deformed pure titanium at high temperatures, Mater. Des. 53 (2014) 749–757, doi:10.1016/j.matdes.2013.07.057.
[15] S. Zhang, Y.C. Wang, A.P. Zhilyaev, D.V. Gunderov, S. Li, G.I. Raab, E. Korznikova, T.G. Langdon, Effect of temperature on microstructural stabilization and mechanical properties in the dynamic testing of nanocrystalline pure Ti, Mater. Sci. Eng. A. 634 (2015) 64–70, doi:10.1016/j.msea.2015.03.032.
[16] H.W. Höppel, L. May, M. Prell, M. Göken, Influence of grain size and precipitation state on the fatigue lives and deformation mechanisms of CP aluminium and AA6082 in the VHCF-regime, Int. J. Fatigue 33 (2011) 10–18, doi:10.1016/J.IJFATIGUE.2010.04.013.
[17] L.R. Saitova, H.W. Höppel, M. Göken, I.P. Semenova, G.I. Raab, Fatigue behavior of ultrafine-grained Ti–6Al–4V 'ELI' alloy for medical applications, Mater. Sci. Eng. A 503 (2009) 145–147, doi:10.1016/J.MSEA.2008.04.082.
[18] L.R. Saitova, H.W. Höppel, M. Göken, I.P. Semenova, R.Z. Valiev, Cyclic deformation behavior and fatigue lives of ultrafine-grained Ti-6AL-4V ELI alloy for medical use, Int. J. Fatigue 31 (2009) 322–331, doi:10.1016/J.IJFATIGUE.2008.08.007.
[19] A.Y. Vinogradov, V.V. Stolyarov, S. Hashimoto, R.Z. Valiev, Cyclic behavior of ultrafine-grain titanium produced by severe plastic deformation, Mater. Sci. Eng. A 318 (2001) 163–173, doi:10.1016/S0921-5093(01)01262-X.
[20] W.-J. Kim, C.-Y. Hyun, H.-K. Kim, Fatigue strength of ultrafine-grained pure Ti after severe plastic deformation, Scr. Mater. 54 (2006) 1745–1750, doi:10.1016/j.scriptamat.2006.01.042.
[21] I.P. Semenova, G.K. Salimgareeva, V.V. Latysh, T. Lowe, Enhanced fatigue strength of commercially pure Ti processed by severe plastic deformation, Mater. Sci. Eng. A. 503 (2009) 92–95, doi:10.1016/j.msea.2008.07.075.
[22] A. Czerwinski, R. Lapovok, D. Tomus, Y. Estrin, A. Vinogradov, The influence of temporary hydrogenation on ECAP formability and low cycle fatigue life of CP titanium, J. Alloys Compd. 509 (2011) 2709–2715, doi:10.1016/j.jallcom.2010.11.188.
[23] P. Lukáš, L. Kunz, L. Navrátilová, O. Bokůvka, Fatigue damage of ultrafine-grain copper in very-high cycle fatigue region, Mater. Sci. Eng. A. 528 (2011) 7036–7040, doi:10.1016/J.MSEA.2011.06.001.
[24] L. Kunz, P. Lukáš, M. Svoboda, Fatigue strength, microstructural stability and strain localization in ultrafine-grained copper, Mater. Sci. Eng. A. 424 (2006) 97–104, doi:10.1016/J.MSEA.2006.02.029.
[25] H.W. Höppel, M. Prell, L. May, M. Göken, Influence of grain size and precipitates on the fatigue lives and deformation mechanisms in the VHCF-regime, Procedia Eng. 2 (2010) 1025–1034, doi:10.1016/J.PROENG.2010.03.111.
[26] P. Lukáš, L. Kunz, M. Svoboda, Fatigue notch sensitivity of ultrafine-grained copper, Mater. Sci. Eng. A 391 (2005) 337–341, doi:10.1016/J.MSEA.2004.09.052.
[27] S.V. Sajadifar, C. Atli, G.G. Yapici, Effect of severe plastic deformation on the damping behavior of titanium, Mater. Lett. 244 (2019) 100–103, doi:10.1016/J.MATLET.2019.02.010.
[28] H. Kitahara, K. Uchikado, J. Makino, N. Iida, M. Tsushida, N. Tsuji, S. Ando, H. Tonda, Fatigue crack propagation behavior in commercial purity Ti severely deformed by accumulative roll bonding process, Mater. Trans. 49 (2008) 64–68, doi:10.2320/matertrans.ME200716.
[29] J. Zhang, S.A.A. Shah, Y. Hao, S. Li, R. Yang, Weak fatigue notch sensitivity in a biomedical titanium alloy exhibiting nonlinear elasticity, Sci. China Mater. 61 (2018) 537–544, doi:10.1007/s40843-017-9158-7.
[30] M. Delshadmanesh, G. Khatibi, M.Z. Ghomsheh, M. Lederer, M. Zehetbauer, H. Danninger, Influence of microstructure on fatigue of biocompatible β-phase Ti-45Nb, Mater. Sci. Eng. A. 706 (2017) 83–94, doi:10.1016/J.MSEA.2017.08.098.
[31] T. Niendorf, F. Rubitschek, H.J. Maier, D. Canadinc, I. Karaman, On the fatigue crack growth–microstructure relationship in ultrafine-grained interstitial-free steel, J. Mater. Sci. 45 (2010) 4813–4821, doi:10.1007/s10853-010-4511-7.
[32] S. Fintová, M. Arzaghi, I. Kuběna, L. Kunz, C. Sarrazin-Baudoux, Fatigue crack propagation in UFG Ti grade 4 processed by severe plastic deformation, Int. J. Fatigue. (2017), doi:10.1016/j.ijfatigue.2017.01.028.
[33] L. Collini, Fatigue crack growth in ECAPed commercially pure UFG copper, Procedia Eng. 2 (2010) 2065–2074, doi:10.1016/J.PROENG.2010.03.222.
[34] H. Mughrabi, On "multi-stage" fatigue life diagrams and the relevant life-controlling mechanisms in ultrahigh-cycle fatigue, Fatigue Fract. Eng. Mater. Struct. 25 (2002) 755–764, doi:10.1046/j.1460-2695.2002.00550.x.

[35] T. Niendorf, D. Canadinc, H.J. Maier, Fatigue damage evolution in ultra-fine-grained interstitial-free steel, Adv. Eng. Mater. 13 (2011) 275–280, doi:10.1002/adem.201000272.
[36] T. Niendorf, J. Dadda, D. Canadinc, H.J. Maier, I. Karaman, Monitoring the fatigue-induced damage evolution in ultrafine-grained interstitial-free steel utilizing digital image correlation, Mater. Sci. Eng. A. 517 (2009) 225–234, doi:10.1016/J.MSEA.2009.04.053.
[37] A. Vinogradov, S. Nagasaki, V. Patlan, K. Kitagawa, M. Kawazoe, Fatigue properties of 5056 Al-Mg alloy produced by equal-channel angular pressing, Nanostruct. Mater. 11 (1999) 925–934, doi:10.1016/S0965-9773(99)00392-X.
[38] T. Niendorf, D. Canadinc, H.J. Maier, I. Karaman, On the microstructural stability of ultrafine-grained interstitial-free steel under cyclic loading, Metall. Mater. Trans. A. 38 (2007) 1946–1955, doi:10.1007/s11661-007-9154-1.
[39] T. Niendorf, D. Canadinc, H.J. Maier, I. Karaman, The role of grain size and distribution on the cyclic stability of titanium, Scr. Mater. 60 (2009) 344–347, doi:10.1016/j.scriptamat.2008.10.033.
[40] S.V. Sajadifar, G.G. Yapici, E. Demler, P. Krooß, T. Wegener, H.J. Maier, T. Niendorf, Cyclic deformation response of ultra-fine grained titanium at elevated temperatures, Int. J. Fatigue 122 (2019) 228–239, doi:10.1016/J.IJFATIGUE.2019.01.021.
[41] M.P. Echlin, J.C. Stinville, V.M. Miller, W.C. Lenthe, T.M. Pollock, Incipient slip and long range plastic strain localization in microtextured Ti-6Al-4V titanium, Acta Mater. 114 (2016) 164–175, doi:10.1016/J.ACTAMAT.2016.04.057.
[42] M.G. Glavicic, V. Venkatesh, Integrated computational materials engineering of titanium: current capabilities being developed under the metals affordability initiative, JOM 66 (2014) 1310–1320, doi:10.1007/s11837-014-1013-0.
[43] F. Bridier, P. Villechaise, J. Mendez, Slip and fatigue crack formation processes in an α/β titanium alloy in relation to crystallographic texture on different scales, Acta Mater. 56 (2008) 3951–3962, doi:10.1016/J.ACTAMAT.2008.04.036.
[44] L. Germain, N. Gey, M. Humbert, P. Vo, M. Jahazi, P. Bocher, Texture heterogeneities induced by subtransus processing of near α titanium alloys, Acta Mater. 56 (2008) 4298–4308, doi:10.1016/J.ACTAMAT.2008.04.065.
[45] J.C. Stinville, F. Bridier, D. Ponsen, P. Wanjara, P. Bocher, High and low cycle fatigue behavior of linear friction welded Ti–6Al–4V, Int. J. Fatigue 70 (2015) 278–288, doi:10.1016/J.IJFATIGUE.2014.10.002.

Autorenversion von: S.V. Sajadifar, T. Wegener, G.G. Yapici, T. Niendorf,: Effect of grain size on the very high cycle fatigue behavior and notch sensitivity of titanium, Theoretical and Applied Fracture Mechanics, Volume 104, 2019, 102362, https://doi.org/10.1016/j.tafmec.2019.102362